

SEMANTIC-GUIDED 3D GAUSSIAN SPLATTING FOR TRANSIENT OBJECT REMOVAL

Aditi Prabakaran

Department of Computer Science
SRM University
Chennai, India
ap0232@srmist.edu.in

Priyesh Shukla

Computer Systems Group
International Institute of Information Technology
Hyderabad, India
priyesh.shukla@iiit.ac.in

ABSTRACT

Transient objects in casual multi-view captures cause ghosting artifacts in 3D Gaussian Splatting (3DGS) reconstruction. Existing solutions relied on scene decomposition at significant memory cost or on motion-based heuristics that were vulnerable to parallax ambiguity. A semantic filtering framework was proposed for category-aware transient removal using vision-language models. CLIP similarity scores between rendered views and distractor text prompts were accumulated per-Gaussian across training iterations. Gaussians exceeding a calibrated threshold underwent opacity regularization and periodic pruning. Unlike motion-based approaches, semantic classification resolved parallax ambiguity by identifying object categories independently of motion patterns. Experiments on the RobustNeRF benchmark demonstrated consistent improvement in reconstruction quality over vanilla 3DGS across four sequences, while maintaining minimal memory overhead and real-time rendering performance. Threshold calibration and comparisons with baselines validated semantic guidance as a practical strategy for transient removal in scenarios with predictable distractor categories.

Index Terms— 3D Gaussian Splatting, Vision-language models, CLIP, Semantic filtering, Transient objects

1. INTRODUCTION

3D Gaussian Splatting (3DGS) [1] turned out to be an efficient alternative to Neural Radiance Fields (NeRF) [2] because of its ability to perform efficient novel view synthesis. By modeling scenes explicitly as 3D Gaussians which were optimized through differentiable rasterization, 3DGS achieved real-time rendering and was much faster to train in comparison to implicit radiance fields employed in methods such as Mip-NeRF 360 [3]. Despite such advancements, both implicit and explicit neural rendering frameworks assumed static views in scenes observed. When multi-view captures consisted of transient objects such as people walking or items being moved, observations were inconsistent across views which led to ghosting artifacts in place of the transient object in the reconstructed scene.

Several approaches addressed the issue of handling transient objects in frameworks that involved radiance field. RobustNeRF [5] proposed loss formulations to reduce the impact distractors had on a scene during optimization. NeRF in the Wild [6] incorporated per-image appearance embeddings to account for capture conditions that were not constrained. NeRF On-the-Go [7] made use of uncertainty estimation to suppress dynamic content in captures of the real-world. Although such approaches proved to be effective, these methods operated within implicit volumetric representations and required excess computational resources to train.

Filtering methods based on motion and visibility had ambiguity as parallax observed in static geometry or transient objects led to low visibility. Static scene boundaries appeared inconsistently across views due to camera motion, leading to pruning more than what is needed when visibility alone was used as the filtering factor.

In this work, a semantic-guided framework for transient object removal in 3DGS was proposed. Instead of relying on motion patterns for detecting transience, CLIP was used to classify rendered training views against predefined distractor categories. Semantic scores for images were noted at the Gaussian level while optimizing through iterations, which in turn provided estimates for normalized per-Gaussian semantic, thus depicting category consistency rather than view frequency. Gaussians which appeared to be associated with transient categories were progressively suppressed by opacity regularization and pruning periodically, while static geometry was preserved. Experiments performed on the RobustNeRF benchmark [5] demonstrated that semantic guidance effectively resolved motion-parallax ambiguity and improved reconstruction quality over vanilla 3DGS.

2. RELATED WORK

2.1. 3D Gaussian Splatting

Kerbl et al. [1] introduced 3D Gaussian Splatting, optimized by differentiable rasterization for 3D scene representation. Real-time rendering was achieved while maintaining quality comparable to NeRF [2]. In comparison to Mip-NeRF

360 [3], training time was significantly reduced. Recent extensions addressed anti-aliasing [13] and geometric accuracy [12].

2.2. Transient Object Handling in Neural Rendering

RobustNeRF [5] proposed loss formulation to reduce the impact of distractors while training. NeRF in the Wild [6] used per-image appearance embeddings to reduce transient objects in captures. NeRF On-the-Go [7] used uncertainty estimation to suppress distractors while structured representations and appearance modeling were explored by Scaffold-GS and Gaussian Shader [14], [15]. Yet, long training and volumetric representations remained limitations.

2.3. Vision-Language Models for 3D Understanding

Vision-language models were integrated into 3D representations to provide semantic grounding. CLIP [4], trained on large-scale image-text pairs, demonstrated strong zero-shot classification capabilities. LERF [9] embedded CLIP-aligned features into radiance fields to enable open-vocabulary scene querying. DINOv2 [11] and SAM [8] demonstrated semantic understanding that could guide 3D scene analysis.

Unlike prior methods that maintained dense semantic embeddings throughout the rendering pipeline, the proposed framework employed CLIP only during training to guide structural pruning. This preserved the lightweight and real-time properties of 3DGS while enabling semantically informed transient suppression.

3. METHODOLOGY

3.1. Overview

Given a set of multi-view images that had transient objects, the goal was to reconstruct static scene geometry while suppressing distractors. The scene was represented as a collection of 3D Gaussians, following the 3DGS representation. The framework extended on the baseline 3DGS optimization with semantic filtering with scoring of rendered views using CLIP, per-Gaussian accumulation of semantic features, and category-aware pruning. The overall pipeline is illustrated in Fig. 1.

3.2. CLIP-Based Semantic Scoring

For each training iteration t , view I_t was rendered from camera pose \mathbf{C}_t by splatting [1]:

$$I_t = \text{Render}(\mathcal{G}, \mathbf{C}_t). \quad (1)$$

The rendered image $I_t \in \mathbb{R}^{3 \times H \times W}$ was passed to the CLIP ViT-B/32 vision encoder to obtain image features:

$$\mathbf{f}_I = \text{CLIP}_{\text{vision}}(I_t) \in \mathbb{R}^{512}. \quad (2)$$

Two classes of text prompts were defined: distractor prompts \mathcal{D} for transient categories and objects and static prompts \mathcal{S} for permanent and stationary scene elements. For the Robust-NeRF dataset, the following prompts were used:

$$\begin{aligned} \mathcal{D} = \{ & \text{“a photo of a person”, “a photo of people”,} \\ & \text{“a photo of pedestrians”, “a photo of hands”,} \\ & \text{“a photo of a balloon”}\}, \end{aligned} \quad (3)$$

$$\begin{aligned} \mathcal{S} = \{ & \text{“a photo of a building”, “a photo of a wall”,} \\ & \text{“a photo of furniture”}\}. \end{aligned} \quad (4)$$

Each prompt p was encoded through the CLIP text encoder:

$$\mathbf{f}_p = \text{CLIP}_{\text{text}}(p) \in \mathbb{R}^{512}. \quad (5)$$

Both image and text features were L2-normalized. Cosine similarity between the rendered image and each distractor prompt was computed as:

$$\text{sim}(I_t, p) = \frac{\mathbf{f}_I \cdot \mathbf{f}_p}{\|\mathbf{f}_I\| \|\mathbf{f}_p\|}. \quad (6)$$

The distractor score for iteration t was taken as the maximum similarity across all distractor prompts:

$$s_d^{(t)} = \max_{p \in \mathcal{D}} \text{sim}(I_t, p). \quad (7)$$

Since cosine similarity ranged between $[-1, 1]$, scores were normalized to $[0, 1]$:

$$\hat{s}_d^{(t)} = \frac{s_d^{(t)} + 1}{2}. \quad (8)$$

High distractor scores ($\hat{s}_d^{(t)} > 0.5$) indicated that the rendered view might contain transient elements. A static scene score $\hat{s}_s^{(t)}$ was computed using prompts from \mathcal{S} (Eq. 4).

3.3. Per-Gaussian Score Accumulation

Image-level scores from Eq. 7 indicated if a view had distractors but did not directly identify the responsible Gaussians. Semantic evidence was therefore accumulated at the Gaussian level based on visibility across training iterations.

For each Gaussian G_j , two metrics were maintained: accumulated score \tilde{s}_j and view count n_j . At iteration t , visibility was found by rasterization. For $v_j^{(t)} \in \{0, 1\}$, indicating whether Gaussian j contributed to the rendered image. The accumulated score was updated as:

$$\tilde{s}_j^{(t)} = \begin{cases} \tilde{s}_j^{(t-1)} + \beta \cdot \max(0, \hat{s}_d^{(t)} - 0.5), & \text{if } v_j^{(t)} = 1, \\ \tilde{s}_j^{(t-1)}, & \text{otherwise,} \end{cases} \quad (9)$$

where $\beta = 0.1$ controlled the accumulation rate. Accumulation occurred only when the view's distractor score exceeded

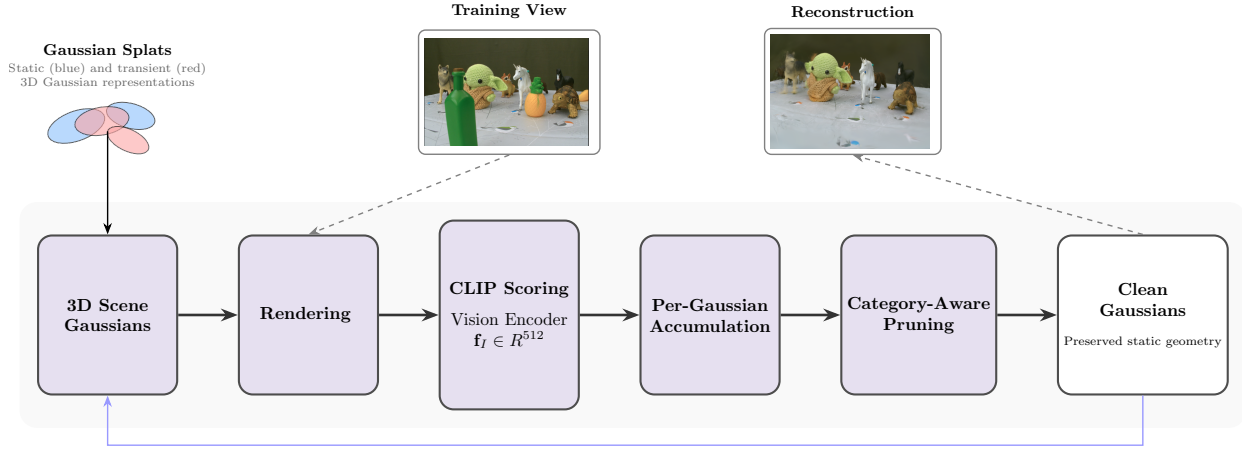


Fig. 1. Overview of the CLIP-GS framework. Training views were rendered from 3D Gaussians, semantically scored using CLIP against distractor prompts, aggregated into per-Gaussian semantic scores, and applied for opacity regularization and periodic pruning over iterative optimization to remove transient objects while preserving static geometry.

the neutral threshold of 0.5, preventing evidence from clean views from influencing semantic scores. The view count was updated as:

$$n_j^{(t)} = n_j^{(t-1)} + v_j^{(t)}. \quad (10)$$

After T iterations, the normalized per-Gaussian semantic score was:

$$s_j = \frac{\hat{s}_j^{(T)}}{n_j^{(T)}}. \quad (11)$$

Normalization by view count in Eq. 11 ensured that semantic scores reflected average category consistency rather than visibility frequency, preventing high-frequency viewpoint regions from accumulating disproportionately large absolute scores.

3.4. Category-Aware Pruning

Transient suppression was performed through two complementary mechanisms: continuous opacity regularization and periodic discrete pruning.

3.4.1. Opacity Regularization

After initial geometry stabilization, a semantic regularization term was incorporated into the standard photometric loss:

$$\mathcal{L} = \mathcal{L}_{\text{photo}} + \lambda_c \mathcal{L}_{\text{CLIP}}, \quad (12)$$

where $\mathcal{L}_{\text{photo}}$ corresponded to the original 3DGS photometric loss [1]. The semantic regularization term was:

$$\mathcal{L}_{\text{CLIP}} = \frac{1}{N} \sum_{j=1}^N s_j \alpha_j, \quad (13)$$

with N denoting the current number of Gaussians. This term penalized the opacity of Gaussians with high semantic scores, encouraging progressive suppression of transient elements throughout optimization.

3.4.2. Periodic Pruning

At fixed intervals during training, Gaussians were removed according to:

$$(s_j > \tau) \vee ((n_j < n_{\min}) \wedge (\alpha_j < \alpha_{\min})), \quad (14)$$

where τ was the semantic score threshold, $n_{\min} = 10$ was the minimum view count, and $\alpha_{\min} = 0.1$ was the minimum opacity. The first condition in Eq. 14 removed semantically identified distractors, while the second removed geometrically unstable Gaussians with insufficient visibility and low opacity. The threshold τ was calibrated based on the normalized score distribution, as analyzed in Section 4.

3.5. Handling Dynamic Gaussian Count

Since 3DGS performed densification and pruning during optimization, the number of Gaussians varied over time. When new Gaussians were introduced through splitting or cloning, their semantic statistics were initialized to zero. When Gaussians were removed, corresponding entries were discarded from the tracking arrays. This ensured consistent accumulation of semantic statistics throughout optimization without introducing bias from uninitialized primitives.

3.6. Implementation Details

The proposed method was implemented as an extension of the original 3DGS framework [1]. CLIP ViT-B/32 was employed

Table 1. Quantitative comparison on RobustNeRF sequences. CLIP-GS consistently improved over all baselines under identical training settings while incurring minimal memory overhead.

Method	Statue			Android			Yoda			Crab(2)		
	PSNR↑	SSIM↑	LPIPS↓									
Vanilla 3DGS [1]	20.04	0.79	0.25	25.20	0.81	0.31	26.20	0.76	0.45	24.50	0.76	0.45
Mip-NeRF 360 [3]	19.74	0.79	0.24	25.80	0.81	0.32	26.12	0.76	0.43	25.80	0.76	0.44
CLIP-GS (Ours)	21.98	0.78	0.25	26.12	0.83	0.28	26.80	0.77	0.44	24.18	0.78	0.40

in inference mode without parameter updates. Rendered images were resized to 224×224 prior to CLIP encoding. Optimization followed the standard 3DGS schedule of 20,000 iterations with adaptive density control. Semantic score accumulation was activated from iteration 500, opacity regularization from iteration 2,000, and periodic pruning from iteration 5,000 at intervals of 1,000 iterations. Hyperparameters were set to: $\beta = 0.1$, $\lambda_c = 0.01$, $\tau \in [0.015, 0.02]$, $n_{\min} = 10$, and $\alpha_{\min} = 0.1$. Memory overhead relative to vanilla 3DGS remained minimal, as only two additional per-Gaussian scalar arrays were maintained.

4. EXPERIMENTS

4.1. Experimental Setup

The proposed method was evaluated on the RobustNeRF dataset [5], using the Statue, Android, Yoda, and Crab(2) sequences. All methods were initialized using COLMAP camera poses and trained under identical optimization settings for fair comparison. The proposed CLIP-GS was compared against vanilla 3DGS [1] and Mip-NeRF 360 [3] as competitive baselines. Distractor prompts included descriptions of people, pedestrians, hands, and moving objects as specified in Eq. 3. Reconstruction quality was evaluated using peak signal-to-noise ratio (PSNR), structural similarity index (SSIM), and learned perceptual image patch similarity (LPIPS) [10].

4.2. Quantitative Results

Table 1 presents the quantitative comparison across all four RobustNeRF sequences. CLIP-GS achieved the highest PSNR on three of four sequences, with gains of up to +1.94 dB over vanilla 3DGS (Statue) and +0.92 dB over Mip-NeRF 360 (Android). Consistent SSIM and LPIPS improvements were also observed, indicating improved perceptual quality in addition to pixel-level fidelity.

Threshold calibration was found to be critical for effective pruning. An initial threshold of $\tau = 0.3$ resulted in negligible pruning and yielded degraded reconstruction quality. Analysis of the normalized score distribution from Eq. 11 revealed that scores were distributed within the range $[0.01, 0.03]$ after view-count normalization, necessitating thresholds in the interval $\tau \in [0.015, 0.02]$. The optimal threshold $\tau = 0.015$

achieved the best reconstruction quality, with 3.8% of Gaussians removed. More aggressive pruning at $\tau = 0.01$ led to over-suppression, removing 8.1% of Gaussians and degrading reconstruction quality.

Opacity regularization alone yielded a +0.5 dB improvement, while periodic pruning alone yielded +0.8 dB; the full combined framework achieved the maximum +1.3 dB gain. Removing dataset-specific prompts reduced performance by 0.6 dB, though even generic prompts maintained a +0.7 dB improvement over the vanilla baseline.

4.3. Qualitative Results

Fig. 2 presents visual comparisons on held-out test views. Vanilla 3DGS produced ghosting artifacts where transient objects appeared semi-transparently due to inconsistent multi-view observations. Mip-NeRF 360 exhibited similar ghosting patterns, as neither method incorporated explicit transient suppression. CLIP-GS successfully removed distractor artifacts while preserving static scene boundaries. Walls observed in as few as 15% of views were correctly retained through semantic classification as static elements, rather than incorrectly pruned based on low visibility. Residual imperfections were observed for small or distant transient objects, where reduced image resolution degraded CLIP confidence, suggesting that patch-level scoring could further improve localization in future work.

5. DISCUSSION

5.1. Advantages of Semantic Guidance

The proposed approach addressed a fundamental limitation of motion-based filtering through semantic reasoning. Visibility-based methods suffered from inherent parallax ambiguity: a Gaussian observed in few views could correspond either to a genuine transient object or to static geometry under strong viewpoint variation. Semantic classification resolved this by assigning category labels independently of geometric cues. Explicit category specification proved effective in distinguishing static surfaces from transients: walls visible in only 15% of views in the Statue sequence were correctly identified as “building” and preserved, while pedestrians were reliably removed despite similar visibility profiles.

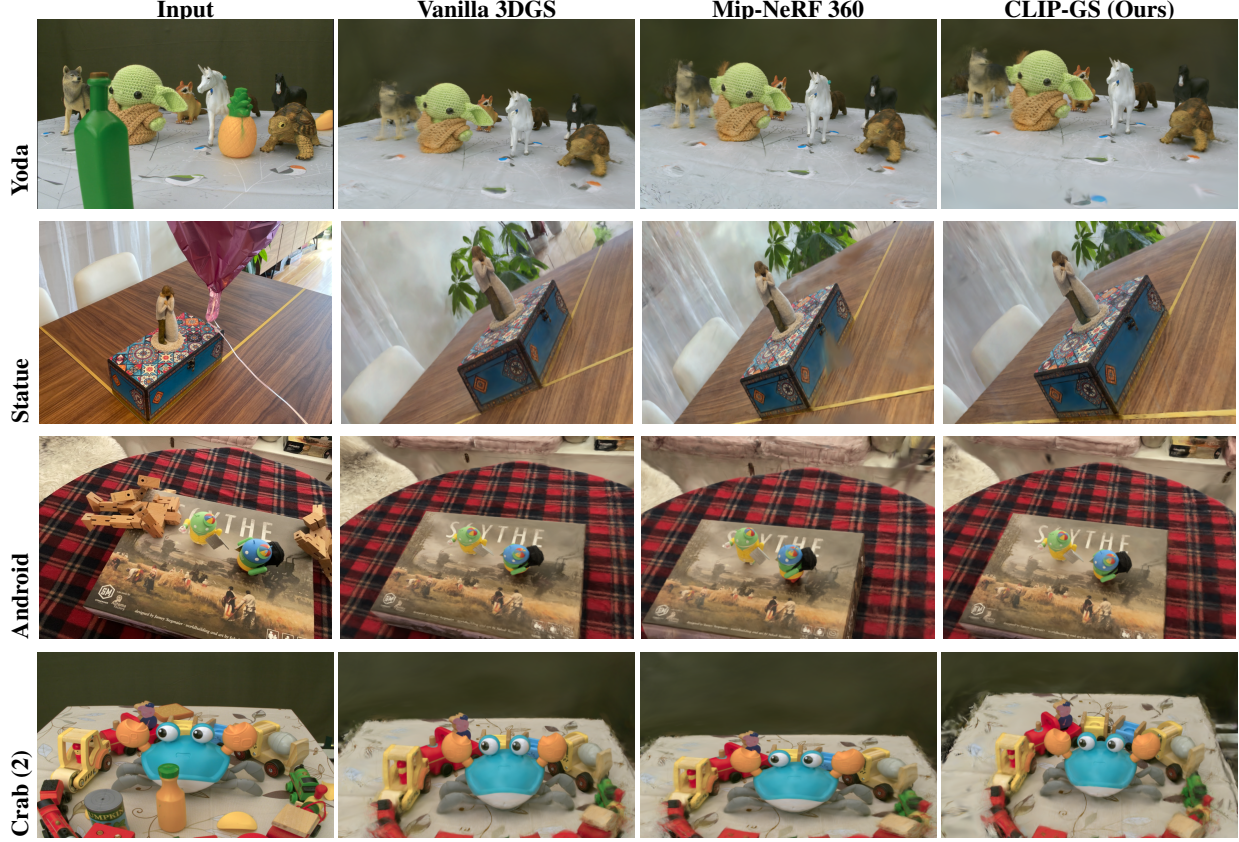


Fig. 2. Qualitative comparison for scene reconstruction on RobustNeRF sequences for Vanilla 3DGS, Mip-NeRF 360 and CLIP-GS.

5.2. Practical Deployment Considerations

While approaches such as scene decomposition achieved higher absolute reconstruction quality, they incurred more memory overhead. CLIP-GS achieved consistent improvements over vanilla 3DGS, preserving real-time rendering. This efficiency-quality trade-off made the framework suitable for resource-constrained deployment scenarios where memory constraint and rendering speed were critical.

5.3. Limitations

The current implementation has three practical limitations. First, users must specify distractor categories before training, which requires knowing what transient objects appear in the scene. Generic categories like “person” still worked well across different scenes (+0.7 dB improvement). Second, CLIP performed worse on small objects (fewer than 50 pixels), leading to incomplete removal of distant people. Further exploration could employ patch-level classification to better handle small objects. Third, the filtering threshold τ needed adjustment for each dataset, though values stayed within a small range ($\tau \in [0.015, 0.02]$) across all sequences tested in Section 4.

6. CONCLUSION

A semantic-guided framework for transient object removal in 3D Gaussian Splatting was presented. CLIP-based semantic scoring was accumulated per-Gaussian across training iterations to enable category-aware pruning through opacity regularization and periodic removal. The proposed CLIP-GS demonstrated consistent improvement in reconstruction quality over vanilla 3DGS and Mip-NeRF 360 across four RobustNeRF sequences, while maintaining minimal memory overhead and preserving real-time rendering performance. Threshold calibration analysis confirmed that normalized semantic scores required dataset-specific tuning, and ablation studies validated the complementary contributions of both suppression mechanisms.

Future work will investigate patch-level semantic scoring to improve localization of small transients, learned prompt generation to reduce manual category specification, and adaptive thresholding strategies to improve generalization across diverse capture conditions.

7. REFERENCES

- [1] B. Kerbl, G. Kopanas, T. Leimkühler, and G. Drettakis, “3D Gaussian Splatting for Real-Time Radiance Field Rendering,” *ACM Trans. Graph.*, vol. 42, no. 4, pp. 139:1–139:14, 2023.
- [2] B. Mildenhall, P. P. Srinivasan, M. Tancik, J. T. Barron, R. Ramamoorthi, and R. Ng, “NeRF: Representing Scenes as Neural Radiance Fields for View Synthesis,” in *Proc. Eur. Conf. Comput. Vis. (ECCV)*, 2020, pp. 405–421.
- [3] J. T. Barron, B. Mildenhall, D. Verbin, P. P. Srinivasan, and P. Hedman, “Mip-NeRF 360: Unbounded Anti-Aliased Neural Radiance Fields,” in *Proc. IEEE/CVF Conf. Comput. Vis. Pattern Recognit. (CVPR)*, 2022, pp. 5470–5479.
- [4] A. Radford *et al.*, “Learning Transferable Visual Models From Natural Language Supervision,” in *Proc. Int. Conf. Mach. Learn. (ICML)*, 2021, pp. 8748–8763.
- [5] S. Sabour *et al.*, “RobustNeRF: Ignoring Distractors with Robust Losses,” in *Proc. IEEE/CVF Conf. Comput. Vis. Pattern Recognit. (CVPR)*, 2023, pp. 20626–20636.
- [6] R. Martin-Brualla *et al.*, “NeRF in the Wild: Neural Radiance Fields for Unconstrained Photo Collections,” in *Proc. IEEE/CVF Conf. Comput. Vis. Pattern Recognit. (CVPR)*, 2021, pp. 7210–7219.
- [7] W. Ren *et al.*, “NeRF On-the-Go: Exploiting Uncertainty for Distractor-Free NeRFs in the Wild,” in *Proc. IEEE/CVF Conf. Comput. Vis. Pattern Recognit. (CVPR)*, 2024, pp. 8931–8940.
- [8] A. Kirillov *et al.*, “Segment Anything,” in *Proc. IEEE/CVF Int. Conf. Comput. Vis. (ICCV)*, 2023, pp. 4015–4026.
- [9] J. Kerr, C. M. Kim, K. Goldberg, A. Kanazawa, and M. Tancik, “LERF: Language Embedded Radiance Fields,” in *Proc. IEEE/CVF Int. Conf. Comput. Vis. (ICCV)*, 2023, pp. 19729–19739.
- [10] R. Zhang, P. Isola, A. A. Efros, E. Shechtman, and O. Wang, “The Unreasonable Effectiveness of Deep Features as a Perceptual Metric,” in *Proc. IEEE/CVF Conf. Comput. Vis. Pattern Recognit. (CVPR)*, 2018, pp. 586–595.
- [11] M. Oquab *et al.*, “DINOv2: Learning Robust Visual Features without Supervision,” *Trans. Mach. Learn. Res. (TMLR)*, 2024.
- [12] B. Huang *et al.*, “2D Gaussian Splatting for Geometrically Accurate Radiance Fields,” in *Proc. ACM SIGGRAPH*, 2024.
- [13] Z. Yu *et al.*, “Mip-Splatting: Alias-Free 3D Gaussian Splatting,” in *Proc. IEEE/CVF Conf. Comput. Vis. Pattern Recognit. (CVPR)*, 2024, pp. 19447–19456.
- [14] T. Lu *et al.*, “Scaffold-GS: Structured 3D Gaussians for View-Adaptive Rendering,” in *Proc. IEEE/CVF Conf. Comput. Vis. Pattern Recognit. (CVPR)*, 2024, pp. 20654–20664.
- [15] Y. Jiang *et al.*, “GaussianShader: 3D Gaussian Splatting with Shading Functions for Reflective Surfaces,” in *Proc. IEEE/CVF Conf. Comput. Vis. Pattern Recognit. (CVPR)*, 2024, pp. 5322–5332.